Ceramics International **22** (1996) 309–315

0272-8842(95)00108-5
0272-8842/96/$15.00

The Diffusionless Cubic-to-Tetragonal Phase Transition in Near-Stoichiometric ZrO_2–CeO_2

S. Torng,[a] K. Miyazawa[b] & T. Sakuma[b]

[a]Chung-Shan Institute of Science and Technology, Materials R and D Center Lung-Tan, Tao-Yuan, Taiwan
[b]Department of Materials Science, Faculty of Engineering, The University of Tokyo, 7-3-1, Hongo, Bunkyo-ku, Tokyo, 113, Japan

(Received 26 June 1995; accepted 24 July 1995)

Abstract: The diffusionless c–t transition of near-stoichiometric ZrO_2–CeO_2 prepared by rapid solidification process in oxygen atmosphere was examined. ZrO_2–CeO_2 with CeO_2 content between 20 and 80 mol% are fully tetragonal and ZrO_2–90 mol%CeO_2 is fully cubic at room temperature. The c–t phase transition is easily completed during rapid cooling. The tetragonality of t-ZrO_2 decreases linearly with increasing CeO_2 content and almost disappears at a composition of about 80 mol%CeO_2. The microstructure of t-ZrO_2 formed by the diffusionless c–t transition in ZrO_2–CeO_2 is characterized by domains with anti-phase boundaries and by twins. The diffusionless c–t transition in near-stoichiometric ZrO_2–CeO_2 is assumed to be a second-order phase transition, as well as that in ZrO_2–Y_2O_3 reported previously, because of the microstructural similarity between the two materials. The nature of the phase transition changes with oxygen deficiency in ZrO_2–CeO_2, which is generated during annealing at high temperatures and/or at low oxygen partial pressure.

1 INTRODUCTION

The diffusionless cubic-to-tetragonal (c–t) phase transition has been extensively studied by various workers, in particular in the ZrO_2–Y_2O_3 system. However, the origin of the c–t transition is still controversial. It has originally been proposed that the diffusionless c–t transition is of martensitic type.[1,2] Heuer and his colleagues have clarified that the microstructure of tetragonal zirconia (t-ZrO_2) formed by this transition is characterized by the domain structure with anti-phase domain boundaries and plate-like or banded twins, and that the transition is very easily completed.[3,4] They called it a first-order, displacive transformation.

In contrast, Sakuma and his co-workers have insisted that the nature of this transition is a second-order phase transition,[5–7] and that the diffusional c–t phase separation accompanies a spinodal.[8,9] The c–t two-phase field in the ZrO_2–Y_2O_3 system is thermodynamically analysed to be a miscibility gap with a sharp maximum and a spinodal from the view point of second-order phase transition.[10] This analysis includes another important assumption that oxygen vacancies introduced for maintaining local electrical neutrality play a major role in the stabilization of cubic zirconia (c-ZrO_2). This assumption must be valid because the same thermodynamic approach is successful to describe the c–t two-phase field in non-stoichiometric ZrO_2.[11]

It is possible to expect that the c–t phase transition will not be affected by oxygen vacancies in binary zirconia alloys containing tetravalent cations, and may easily be understood. However, the experimental results reported in ZrO_2–CeO_2 are not consistent with each other.[12–14] This is probably caused by the reduction of cerium ions from the tetravalent state (+4) to the trivalent state (+3) at high temperatures or at low oxygen partial pressure.[15] In the present study, the c–t transition is examined in near-stoichiometric ZrO_2–CeO_2

without oxygen vacancies, which were prepared by the rapid solidification process (RSP) in oxygen atmosphere.

2 EXPERIMENTAL PROCEDURE

ZrO_2 and CeO_2 powders of 99.9% purity supplied by Rare Metallic Co. Ltd and Wako Pure Chemical Industries Ltd, respectively, were used for starting materials. Binary stoichiometric ZrO_2–CeO_2 with CeO_2 content of 20–90 mol% at intervals of 10 mol% were obtained by melting in oxygen atmosphere using an image furnace. Before melting, the mixed powders were ball-milled and pressed into green compacts of ϕ3 mm x 80 mm in size under a pressure of 200MPa. They were presintered at 1400°C for 3h in air and then melted with an image furnace in an oxygen atmosphere. The samples were rapidly cooled after melting by falling on to a twin roller spinning attachment. Thin films with white colour and a thickness of about 30 μm were obtained. TG (thermogravimetric) analysis was made with Seiko Instruments Inc. model SSC5200 to estimate the oxygen deficiency. XRD (X-ray diffraction) analysis was made with MAC-Science model MXP-18. The Ce content was analysed on free surfaces and also on the central part of the thin films with an EPMA (electron probe microanalyser). Shimadzu EPMA-8750 was used at 15kV and 15nA. Samples for TEM (transmission electron microscopy) were prepared with ion-milling. An electron microscope Hitachi H-800 TEM was used at 200kV.

3 RESULTS

Figure 1 is an SEM image of ZrO_2–40 mol%CeO_2 film obtained with the RSP process. Fine columnar grains are developed nearly perpendicular to the film surfaces. The solidification must start from surfaces to centre. The composition fluctuation of Ce ions detected with EPMA analysis was within $\pm 3.0\%$ in each material. In addition, no weight change could be detected with TG analysis upon heating up to 800°C in oxygen atmosphere. The films must be near-stoichiometric $(Zr_xCe_{1-x})O_2$, because TG analysis is often used to estimate the amount of oxygen vacancies in this system.[15–17]

The XRD analysis has revealed that ZrO_2 containing 20–70 mol%CeO_2 is fully tetragonal at room temperature. Figure 2 is the XRD profile of ZrO_2–40 mol%CeO_2. The 004 and 400 peaks are clearly split, so that this alloy is identified to be

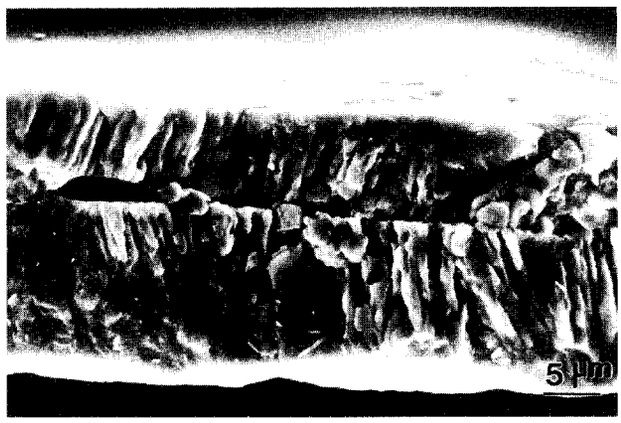

Fig. 1. A photograph of the cross section of ZrO_2–40 mol% CeO_2 film melted in oxygen atmosphere. The film thickness is about 20 μm.

single t-ZrO_2 at room temperature. Other peaks can also be indexed with t-ZrO_2, as demonstrated in Fig. 2.

Figure 3 shows the XRD profile of ZrO_2–80 mol%CeO_2. The profile exhibits a broad and unsymmetrical 004 peak. It may be possible to index the peaks from c-ZrO_2. However, as mentioned later, the weak forbidden reflections for c-ZrO_2 are observed in diffraction patterns in TEM observations. ZrO_2–80 mol%CeO_2 must be t-ZrO_2 with extremely small tetragonality. In contrast, ZrO_2–90 mol%CeO_2, whose XRD profile is shown in Fig. 4, is regarded as c-ZrO_2 with a fluorite structure.

Figure 5 shows the plots of lattice parameter (a) and tetragonality (b) in t-ZrO_2 and c-ZrO_2 as a function of CeO_2 content. The lattice parameters, a_t,c_t for t-ZrO_2 and a_c for c-ZrO_2, increase linearly with an increase of CeO_2 content. The lattice parameters may change continuously from t-ZrO_2 to c-ZrO_2 at about 80 mol%CeO_2, as well as in ZrO_2–M_2O_3 (M: Y, Yb, Sc, Sm, etc.) at about 8 mol%M_2O_3.[18–20] At least, a discontinuous change in lattice parameter with composition from t-ZrO_2 to c-ZrO_2 could not be detected at room temperature. The tetragonality of t-ZrO_2 decreases with increasing CeO_2 content and is close to unity at about 80 mol%CeO_2.

The SADPs (selected area diffraction patterns) in ZrO_2–40 mol%CeO_2 are shown in Fig. 6. The odd/odd/even type reflections arise in the SADPs which are characteristic of t-ZrO_2. Such reflections were observed in ZrO_2–20 ~ 70 mol%CeO_2. Weak odd/odd/even reflections are also observed in ZrO_2–80 mol%CeO_2, as shown in Fig. 7. These materials must be fully tetragonal at room temperature because the reflections always appear in a whole range of samples examined. The results are consistent with those of XRD analysis.

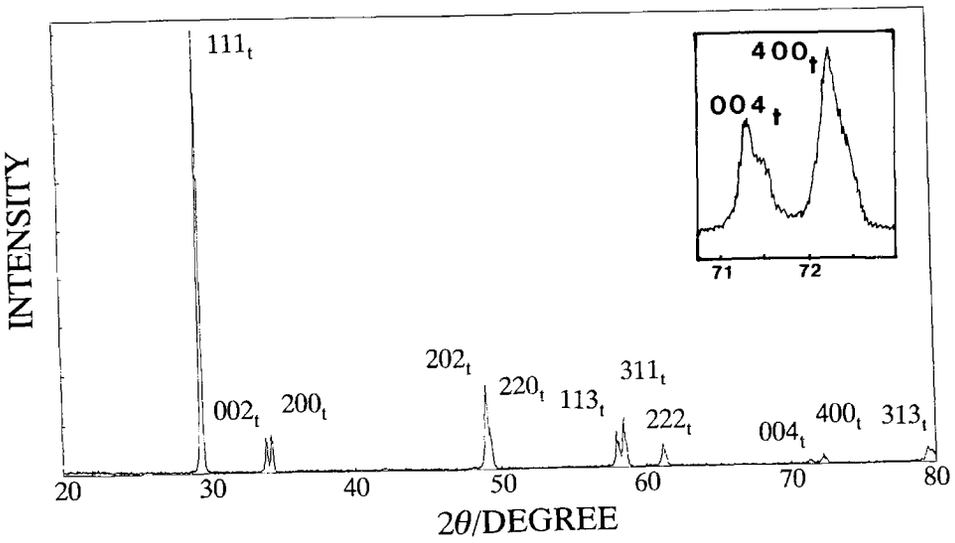

Fig. 2. The XRD profile of ZrO_2–40 mol%CeO_2 melted in oxygen atmosphere.

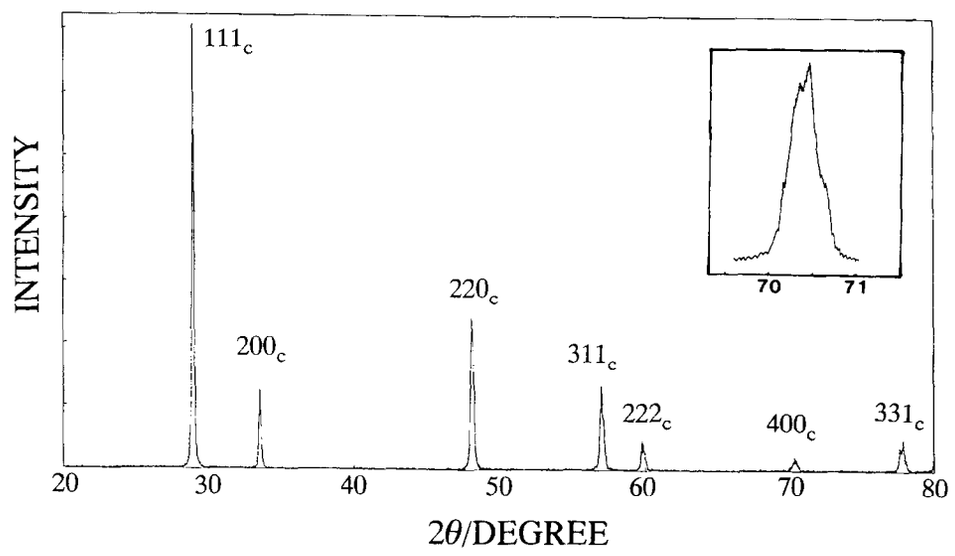

Fig. 3. The XRD profile of ZrO_2–80 mol%CeO_2 melted in oxygen atmosphere.

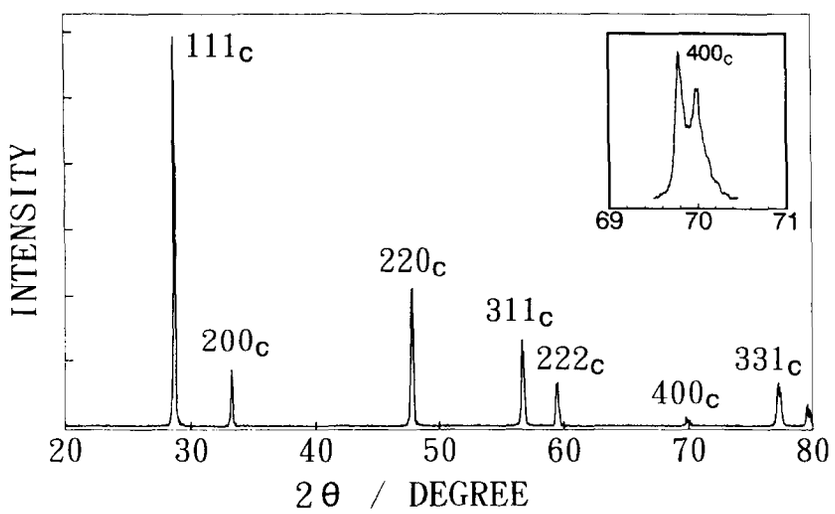

Fig. 4. The XRD profile of ZrO_2–90 mol%CeO_2 melted in oxygen atmosphere.

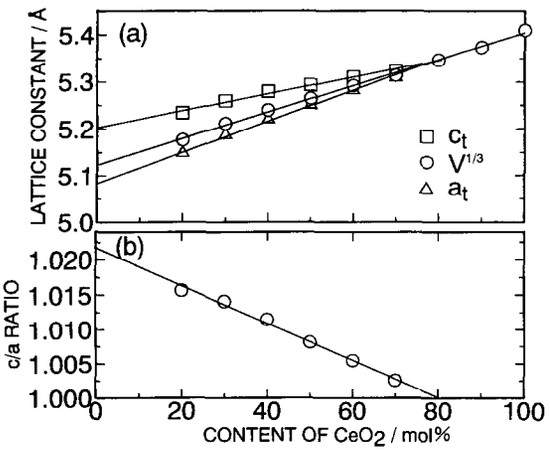

Fig. 5. Plots of (a) lattice parameters and (b) c/a ratio of c-ZrO_2 and t-ZrO_2 as a function of ceria content.

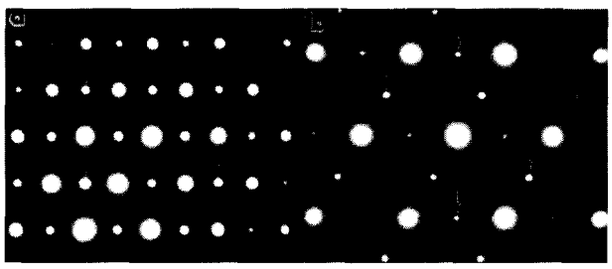

Fig. 6. SADPs of ZrO_2–40 mol%CeO_2 melted in oxygen atmosphere. Beam directions are close to (a)[011] and (b)[111]. Arrows indicate the 112 type reflections which are forbidden for c-ZrO_2.

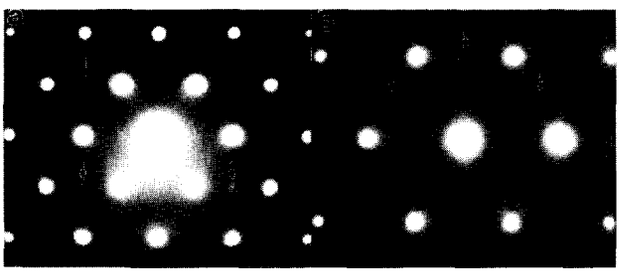

Fig. 7. SADPs of ZrO_2–80 mol%CeO_2 melted in oxygen atmosphere. Beam directions are close to (a)[011] and (b)[111]. Arrows indicate the 112 type reflections which are forbidden for c-ZrO_2.

Figure 8 shows a BF (bright field) image (a) and a DF (dark field) image taken with a 112 reflection (b) in the same area of ZrO_2–20 mol%CeO_2. The herring-bone structure appears in these micrographs. The structure consists of a regular array of transformation twins, and resembles that in ZrO_2–Y_2O_3 containing about 3 mol%Y_2O_3.[21,22]

Plate or lenticular features are developed in ZrO_2–40 ~ 60 mol%CeO_2. An example of the micrographs is shown in Fig. 9. In the dark field image of (b) taken with a 112 reflection, curvilinear boundaries are observed, which are the domain boundaries in t-ZrO_2.[3,4]

Fig. 8. (a) BF and (b) DF images taken with a 112 reflection in ZrO_2–20 mol%CeO_2 melted in oxygen atmosphere.

The microstructures of t-ZrO_2 formed by the diffusionless c–t transition during rapid cooling from the liquid state in ZrO_2–CeO_2 are characterized by the domain structure and transformation twins and are very similar to those of t-ZrO_2 in Y_2O_3-doped ZrO_2.[3–6] The domain structure and twins were observed in a whole range of samples in ZrO_2–CeO_2 containing up to 70 mol%CeO_2. It is again confirmed that these materials are fully tetragonal at room temperature. The microstructure was not clearly found in a dark field image with a 112 reflection in ZrO_2–80 mol%CeO_2 because the intensity of 112 reflections is very weak. However, the weak 112 reflections are always found in ZrO_2–80 mol%CeO_2, so that it must also be fully tetragonal. ZrO_2–90 mol%CeO_2 was almost featureless in bright field images except for a few dislocations, as in ZrO_2–Y_2O_3.[21]

4 DISCUSSION

The experimental data obtained in near-stoichiometric ZrO_2–20 ~ 90 mol%CeO_2 are very similar to those reported in ZrO_2–Y_2O_3. At first, the cube

Fig. 9. (a) BF and (b) DF images taken with a 112 reflection in ZrO_2–40 mol%CeO_2 melted in oxygen atmosphere.

root of unit cell volume changes almost continuously with CeO_2 content from t-ZrO_2 and c-ZrO_2, as shown in Fig. 5(a). Within the accuracy of XRD analysis, the volume change is not detected between c-ZrO_2 and t-ZrO_2 in near-stoichiometric ZrO_2–CeO_2 at a composition of about 80 mol%CeO_2. The tetragonality of t-ZrO_2 decreases continuously with an increase of CeO_2 content, and almost disappears at about 80 mol%CeO_2, as shown in Fig. 5(b). These results are in accordance with those in ZrO_2–M_2O_3 systems.[18–20]

Second, the microstructures of t-ZrO_2 formed by the diffusionless c–t phase transition in stoichiometric ZrO_2–CeO_2 are characterized by the domain structure and transformation twins. The twinned microstructures vary from herring-bone structure to plate or lenticular features with an increase of CeO_2 content. The microstructures are also similar to those reported in ZrO_2–Y_2O_3 prepared by arc-melting.[21] Since there are no or very few oxygen vacancies in near-stoichiometric ZrO_2–CeO_2 in contrast to ZrO_2–Y_2O_3, it is concluded that the microstructures of t-ZrO_2 formed by the diffusionless c–t transition are not influenced by the presence of oxygen vacancies.

Third, stoichiometric ZrO_2–CeO_2 rapidly cooled from high temperatures is fully tetragonal or cubic at room temperature, and the two-phase structure consisting of t-ZrO_2 and c-ZrO_2 could not be detected, as has been clarified in ZrO_2–Y_2O_3.[3–6] All the experimental facts are not contradictory to the assumption that the c–t transition is approximated to be a second-order phase transition as has been proposed by Sakuma and his co-workers.[5–7]

An opposite result was reported by Yashima *et al.*[13] in ZrO_2–CeO_2 obtained by sintering. They claimed that the diffusionless c–t transition is a thermally-activated process and is of a first-order type. This conclusion is derived from the experimental results that c-ZrO_2 is retained in ZrO_2–30 ~ 60 mol%CeO_2 quenched from high temperatures of either 1660 or 1760°C, and is isothermally transformed into t-ZrO_2 during annealing at low temperatures between 200 and 400°C. The isothermal transformation is thought to be controlled by oxygen diffusion.

The retention of c-ZrO_2 at room temperature in ZrO_2–30 ~ 60 mol%CeO_2 must be associated with oxygen vacancies. They reported that their quenched powders have a dark gray colour due to oxygen deficiency. As demonstrated previously,[10] oxygen vacancies stabilize c-ZrO_2, and hence c-ZrO_2 will be retained if a sufficient amount of vacancies are introduced. In fact, it has been reported that about 2% of oxygen vacancies are sufficient to retain c-ZrO_2 at room temperature in ZrO_2–50 mol% CeO_2.[17]

Another controversial point is whether the c–t transition is a thermally-activated process controlled by oxygen diffusion or not. From the experimental data exhibiting the isothermal c–t transition during low temperature annealing in air, it may be concluded that the c–t transition is a first-order phase transition controlled by oxygen diffusion.[13] In this case, oxygen absorption and the resultant decrease in oxygen vacancies in annealed samples must drive the c–t transition. However, it should be noted that oxygen diffusion takes place from surface to interior, and the oxygen vacancy concentration is not kept constant in samples before the oxidation is completed. Therefore, the c–t transition is induced from surfaces to centre during oxidation, and appears as a time-dependent process even if this transition is of a second-order type. The phenomena observed by Yashima *et al.* are not the evidence denying the assumption of the second-order c–t transition in stoichiometric $(Zr,Ce)O_2$.

Due to the intrinsic property of cerium ions, which are easily reduced from Ce^{4+} to Ce^{3+} ions at high temperatures, ZrO_2–CeO_2 prepared by various processes must contain different amounts of oxygen vacancies. The nature of the diffusionless

c–t transition is likely to change with the presence of oxygen vacancies. For example, in non-stoichiometric ZrO_2–CeO_2 with oxygen vacancies of about 9%, c-ZrO_2 has a regular oxygen ion displacement in the <111> direction, and accordingly the c–t transition is regarded as a first-order phase transition.[14,17] In contrast, the results reported in non-stoichiometric ZrO_2–CeO_2 with about 2% oxygen vacancies are rather similar to the present ones.[13,23] We will have to take into account a crucial role of oxygen vacancies to understand the c–t phase transition in ZrO_2–CeO_2.

5 CONCLUSION

The diffusionless c–t phase transition was examined in stoichiometric ZrO_2–CeO_2 prepared by the rapid solidification process in an oxygen atmosphere, and the following results were obtained.

1. ZrO_2–CeO_2 with CeO_2 content of 20–80 mol% are identified to be fully tetragonal at room temperature. The tetragonality of t-ZrO_2 decreases continuously with increasing CeO_2 content. The tetragonality almost disappears at a composition of 80 mol%$CeCO_2$.
2. The c–t phase transition is easily completed during rapid cooling from high temperatures, and the two phase structure consisting of t-ZrO_2 and c-ZrO_2 is not developed.
3. The microstructures of t-ZrO_2 formed by the diffusionless c–t transition in stoichiometric ZrO_2–CeO_2 are characterized by the domain structure and twins. The domains are developed in the whole region of each sample.
4. The experimental results obtained in stoichiometric ZrO_2–CeO_2 are very similar to those reported in ZrO_2–Y_2O_3, and are not inconsistent with the assumption that the c–t phase transition is approximated to be a second-order phase transition.

ACKNOWLEDGEMENT

The authors are grateful to Mr. Nakamura (Faculty of Engineering, The University of Tokyo) for his assistance in TEM observation.

REFERENCES

1. COHEN, I. & SHANER, B. E, A metallographic and X-ray study of the UO_2–ZrO_2 system. *J. Nuclear Mater.*, **9** (1963) 18–52.
2. ANDERSSON, C. A., GREGGI, J., Jr, & GUPTA, T. K., Diffusionless tranformations in zirconia alloys. In *Advances in Ceramics, Vol. 12, Science and Technology of Zirconia II*, ed. N. Claussen, M. Rühle & A. H. Heuer. Am. Ceram. Soc., Columbus, OH, 1984, pp.78–85.
3. LANTERI, V., HEUER, A. H. & MITCHELL, T. E., Tetragonal phase in the system ZrO_2–Y_2O_3. In *Advances in Ceramics, Vol. 12, Science and Technology of Zirconia II*, ed. N. Claussen, M. Rühle & A. H. Heuer. Am. Ceram. Soc., Columbus, OH, 1984, pp.118–30.
4. CHAIM, R., RÜHLE, M. & HEUER, A. H., Microstructural evolution in a ZrO_2–12 wt%Y_2O_3 ceramic. *J. Am. Ceram. Soc.*, **68** (1985) 427–31.
5. SAKUMA, T., Development of the domain structure associated with the diffusionless cubic-to-tetragonal transition in ZrO_2–Y_2O_3 alloys. *J. Mater. Sci.*, **22** (1987) 4470–5.
6. SAKUMA, T. & HATA, H., The domain structure of tetragonal zirconia in ZrO_2–Y_2O_3 alloys. In *Zirconia '88: Advances in Zirconia Science and Technology*, ed. S. Meriani and C. Palmonari. Elsevier Applied Science, London, 1989, pp. 283–92.
7. ZHOU, Y., LEI, T. & SAKUMA, T., Diffusionless cubic-to-tetragonal phase transition and microstructural evolution in sintered zirconia–yttria ceramics. *J. Am. Ceram. Soc.*, **74** (1991) 633–40.
8. SAKUMA, T., YOSHIZAWA, Y. & SUTO, H., The modulated structure formed by isothermal ageing in ZrO_2–5.2 mol%Y_2O_3 alloy. *J. Mater. Sci.*, **20** (1985) 1085–92.
9. SAKUMA, T., YOSHIZAWA, Y. & SUTO, H., Metastable two-phase region in the zirconia-rich part of ZrO_2–Y_2O_3 system. *J. Mater. Sci.*, **21** (1986) 1436–40.
10. HILLERT, M. & SAKUMA, T., Thermodynamic modeling of the c→t transformation in ZrO_2 alloys. *Acta Metall. Mater.*, **39** (1991) 1111–15.
11. HILLERT, M., Thermodynamic model of the cubic–tetragonal transition in non-stoichiometric zirconia. *J. Am. Ceram. Soc.*, **74** (1991) 2005–6.
12. MUROI, T., ECHIGOYA J. I. & SUTO, H., Structure and phase diagram of ZrO_2–CeO_2 ceramics. *Trans. Jpn Inst. Met.*, **29** (1988) 634–41.
13. YASHIMA, M., MORIMOTO, K., ISHIZAWA, N. & YOSHIMURA, M., Zirconia–ceria solid solution synthesis and the temperature–time–transformation diagram for the 1:1 composition. *J. Am. Ceram. Soc.*, **76** (1993) 1745–50.
14. TORNG, S., MIYAZAWA, K. & SAKUMA, T., Microstructure of cubic and tetragonal zirconia in ZrO_2–CeO_2. In *Advanced Materials '93, V/B: Shape Memory Materials and Hidrides*, ed. K. Otsuka *et al. Trans. Mat. Res. Soc. Jpn*, **18B** (1994) 889–92.
15. MASCHIO, S., SBAIZERO, O. & MERIANI, S., Mechanical properties in the ceria–zirconia system. *J. Europ. Ceram. Soc.*, **9** (1992) 127–32.
16. TRIPP, W. C. & TALLAN, N. M., Revised weight change in non-stoichiometric ZrO_2. *J. Am. Ceram. Soc.*, **55** (1972) 60.
17. TORNG, S., MIYAZAWA, K. & SAKUMA, T., Role of oxygen vacancies on cubic–tetragonal phase transition in ZrO_2–CeO_2. *Mater. Sci. Tech.*, **11** (1995) 130–5.
18. YOSHIMURA, M., YASHIMA, M., NOMA, T. & SOMIYA, S., Formation of diffusionlessly transformed tetragonal phases by rapid quenching of melts in ZrO_2–$RO_{1.5}$ systems (R = rare earths). *J. Mater. Sci.*, **25** (1990) 2011–16.
19. SAKUMA, T., Phase transformation and microstructure of partially-stabilized zirconia. *Trans. Jpn Inst. Met.*, **29** (1988) 879–93.
20. SHEU, T., TIEN, T. & CHEN, I., Cubic-to-tetragonal (t') tranformation in zirconia-containing systems. *J. Am. Ceram. Soc.*, **75** (1992) 1108–16.

21. SAKUMA, T., YOSHIZAWA, Y. & SUTO, H., The microstructure and mechanical properties of yttria-stabilized zirconia prepared by arc-melting. *J. Mater. Sci.*, **20** (1985) 2399–407.
22. HAYAKAWA, M., ADACHI, K. & OKA, K., Tweed contrast with (223) habit in arc-melted zirconia–yttria alloys. *Acta Metall. Mater.*, **38** (1990) 1761–67.
23. TORNG, S., MIYAZAWA, K., SUZUKI, K. & SAKAMA, T., The domain structure of cubic zirconia in ZrO_2–O. *Philos. Mag.*, **A70** (1994) 505–17.